



## Perchlorate removal from aqueous solutions by granular ferric hydroxide (GFH)

Eva Kumar<sup>a</sup>, Amit Bhatnagar<sup>a</sup>, Jeong-A Choi<sup>a</sup>, Umesh Kumar<sup>b</sup>, Booki Min<sup>c</sup>, Yongje Kim<sup>d</sup>,  
Hocheol Song<sup>d</sup>, Ki Jung Paeng<sup>e</sup>, Yong Mee Jung<sup>f</sup>, R.A.I. Abou-Shanab<sup>a</sup>, Byong-Hun Jeon<sup>a,\*</sup>

<sup>a</sup> Department of Environmental Engineering, Yonsei University, Wonju, 220-710, South Korea

<sup>b</sup> Department of Chemical Engineering, National Taiwan University, Taipei, 10617, Taiwan

<sup>c</sup> Department of Environmental Science and Engineering, Kyung Hee University, Yongin-Si, 446-701, South Korea

<sup>d</sup> Korea Institute of Geoscience and Mineral Resources, KIGAM, Daejeon, 305-350, South Korea

<sup>e</sup> Department of Chemistry, Yonsei University, Wonju, 220-710, South Korea

<sup>f</sup> Department of Chemistry, Kangwon National University, Chunchon, 200-701, South Korea

### ARTICLE INFO

#### Article history:

Received 8 October 2009

Received in revised form 15 February 2010

Accepted 20 February 2010

#### Keywords:

Perchlorate

Granular ferric hydroxide (GFH)

Kinetics

Adsorption isotherms

Raman spectroscopy

### ABSTRACT

The present research evaluates the efficacy of granular ferric hydroxide (GFH) for perchlorate removal from aqueous solutions. Laboratory scale experiments were conducted to investigate the influence of various experimental parameters such as contact time, initial perchlorate concentration, temperature, pH and competing anions on perchlorate removal by GFH. Results demonstrated that perchlorate uptake rate was rapid and maximum adsorption was completed within first 30 min and equilibrium was achieved within 60 min. Pseudo-second-order model favorably explains the sorption mechanism of perchlorate on to GFH. The maximum sorption capacity of GFH for perchlorate was ca. 20.0 mg g<sup>-1</sup> at pH 6.0–6.5 at room temperature (25 °C). The optimum perchlorate removal was observed between pH range of 3–7. The Raman spectroscopy results revealed that perchlorate was adsorbed on GFH through electrostatic attraction between perchlorate and positively charged surface sites. Results from this study demonstrated potential utility of GFH that could be developed into a viable technology for perchlorate removal from water.

© 2010 Elsevier B.V. All rights reserved.

### 1. Introduction

Perchlorate (ClO<sub>4</sub><sup>-</sup>) is an alarming inorganic contaminant which has been detected in various public drinking water systems throughout the United States [1]. Environmental contamination by perchlorate has also been documented in different Asian countries namely, China [2], Korea [3], and Japan [4]. Perchlorate and its salts are mainly used in missile/rocket propellants and in various industrial applications (e.g. manufacturing of matches, airbag inflators, safety flares, and fireworks) [5,6]. Natural sources of perchlorate have also been reported [7,8]. The major sources of perchlorate contamination in groundwater are due to unsafe disposal of rocket fuel and explosives by the aerospace and chemical industries [9].

The toxic health effects of perchlorate contamination in drinking water are well documented [10]. Eye and skin irritation, cough, nausea, vomiting, and diarrhea are the symptoms of short term exposure to high dosage of perchlorate [11]. Perchlorate exposures for a longer period can result in the inhibition of iodine uptake

in the thyroid gland, affecting/altering the production of thyroid hormones and possibly causing mental retardation in fetuses and infants [12,13]. Considering the human health concerns, perchlorate was included to the drinking water contaminant candidate list in 1998 by U.S. Environmental Protection Agency (US EPA) [14]. The US EPA adopted a new drinking water standard of 24.5 μg L<sup>-1</sup> for perchlorate in 2005 [15]. Perchlorate has received tremendous attention in recent years, mainly due to the challenges faced by the drinking water industry regarding its treatment.

The removal of perchlorate from water has been very challenging for the researchers as perchlorate ions are non-volatile, highly soluble, and kinetically inert in water [5]. Various treatment technologies have been investigated for perchlorate removal from water, e.g. microbial reduction [5,16], reduction by zero-valent iron combined with perchlorate-reducing microorganisms [17,18], ion exchange [19], membrane technologies [20], electrochemical reduction [21] and adsorption [22–26]. The shortcomings of most of these methods are high operational and maintenance costs, secondary pollution and complicated procedure involved in the treatment. Comparatively, adsorption seems to be a more attractive method in terms of cost, simplicity of design and operation. Activated carbon has been found less effective for adsorbing perchlorate in most cases, and needs to be tailored or modified [22,23]. Recently, protonated cross-linked chitosan was also explored to

\* Corresponding author at: Department of Environmental Engineering, Baekun Hall #332, Yonsei University, 234 Maeji Heungeop, Wonju, 220-710, Gangwon-do, South Korea. Tel.: +82 33 760 2446; fax: +82 33 760 2194.

E-mail address: [bhjeon@yonsei.ac.kr](mailto:bhjeon@yonsei.ac.kr) (B.-H. Jeon).

remove perchlorate from water by Xie et al. [25]. The results indicated that the chitosan with cationic modification has a potential for application to perchlorate removal from contaminated water.

In the present study, the feasibility of granular ferric hydroxide (GFH) for perchlorate removal was tested as several iron-based adsorbents that require fewer chemical pretreatments and/or have longer operational lives have been intensively examined for the treatment of arsenic and perchlorate [27,28]. GFH has previously shown promising results for the removal of various anions e.g. arsenic, bromate and fluoride [29,30,31]. To further test the potential of GFH for other anions (perchlorate as a model pollutant), adsorption studies were performed to examine the influence of various experimental parameters such as effect of contact time, initial perchlorate concentration, temperature, pH, and competing anions on perchlorate removal. The data from the experiments were fitted with different kinetic models to identify the adsorption mechanism. The Raman spectroscopic analysis was used to study the perchlorate sorption mechanism onto GFH. The results have been thoroughly discussed to better understand the perchlorate sorption mechanism onto GFH.

## 2. Materials and methods

### 2.1. Materials

GFH was purchased from GEH Wasserchemie (GmbH & Co. KG, Osnabrück, Germany). It is a poorly crystallized  $\beta$ -FeOOH, which is predominantly the mineral akaganeite [32]. It has a specific surface area of 250–300 m<sup>2</sup> g<sup>-1</sup> and porosity of 75–80%. Pore size distribution is similar for all fractions of GFH [33]. A total of 97% of the pores are less than 4.5 nm [34]. The pH of point of zero charge (pH<sub>PZC</sub>) was determined by different researchers to be 7.5–8.0 [29,34]. The material has a grain size range of 0.32–2.0 mm and a water content of 54–60% [32]. All stock solutions were prepared using analytical reagent grade chemicals and deionized water (DI). Perchlorate stock solution was prepared by dissolving NaClO<sub>4</sub> (Sigma–Aldrich, MO, USA) in DI water. Standards and perchlorate spiked samples at a required concentration range were prepared by appropriate dilution of the stock solution with DI water.

### 2.2. Perchlorate analysis

Perchlorate concentration was determined using two Metrohm ion chromatography (IC) systems (Metrohm Ltd., Switzerland). The first one was equipped with Metrohm 858 professional sample processor assembled with 20  $\mu$ L injection loop. The separation column used was Metrosep A Supp5. The mobile phase consisted of 5 mmol L<sup>-1</sup> Na<sub>2</sub>CO<sub>3</sub>, 10 mmol L<sup>-1</sup> NaOH and 20% acetone. Data acquisition was performed using MagIC Net 1.1 program. With this setup, the detection limit for perchlorate was 50  $\mu$ g L<sup>-1</sup>. The other one was equipped with 838 advanced sample processor assembled with 1000  $\mu$ L injection loop. The separation column used was Dual 4-100 column. The mobile phase consisted of 12 mM p-cyanophenol + 5.0 mM LiOH. Data acquisition was performed using MagIC Net 1.1 program. With this setup, the detection limit for perchlorate was 0.5  $\mu$ g L<sup>-1</sup>.

### 2.3. Raman spectroscopic analysis

Raman spectroscopic analysis was performed to provide insight into the mechanism of perchlorate interaction with GFH. Perchlorate spiked solutions were prepared with the concentration range of 20–700 mg L<sup>-1</sup>. The solutions were equilibrated with GFH (1 g L<sup>-1</sup>) for 24 h followed by drying. The samples were analyzed by Raman spectroscopy (LabRAM ARAMIS, HORIBA Jobin Yvon, USA). The laser wavelength used in the Raman measurement was 633 nm.

The exposure time for measurement was 30 s and sample accumulation was done five times.

### 2.4. Adsorption studies

The adsorption of perchlorate on GFH was conducted at room temperature (25  $\pm$  2  $^{\circ}$ C) by batch experiments. Twenty five milliliters of perchlorate solution of varying initial concentrations (50  $\mu$ g L<sup>-1</sup> to 500 mg L<sup>-1</sup>) in 50 mL capped tubes were shaken with 0.025 g of GFH for a specified period of contact time in a temperature controlled shaking assembly (Jeio Tech Co., SWB-20 shaking water bath). After equilibrium, samples were filtered using 0.25  $\mu$ m filters (Versapor, Pall Co., USA) and the perchlorate concentration was measured by ion chromatography. Reproducibility of the measurements was determined in triplicates and the average values are reported. Relative standard deviations were found to be within  $\pm$ 3.0%. The amount of perchlorate adsorbed ( $q_e$  in mg g<sup>-1</sup>) was calculated as follows:

$$q_e = \frac{(C_0 - C_e) \cdot V}{m} \quad (1)$$

where,  $C_0$  and  $C_e$  are the initial and final concentrations of perchlorate in solution (mg L<sup>-1</sup>),  $V$  is the volume of solution (L) and  $m$  is mass of the adsorbent (g).

The effect of contact time (1 min to 24 h) was examined with initial perchlorate concentrations of 5 and 10 mg L<sup>-1</sup>. The effect of equilibrium pH was investigated by adjusting solution pH from 3 to 12 using 0.1 M HCl and 0.1 M NaOH with an initial perchlorate concentration of 20 mg L<sup>-1</sup>. The effects of competing anions (chloride, fluoride, nitrate, bromate, carbonate, sulphate and phosphate) on perchlorate adsorption were investigated by performing perchlorate adsorption under a fixed perchlorate concentration (20 mg L<sup>-1</sup>), and initial competing anion concentrations of 20–100 mg L<sup>-1</sup> with GFH dosage of 1 g L<sup>-1</sup>.

## 3. Results and discussion

### 3.1. Effect of contact time and initial perchlorate concentration

The adsorption of perchlorate on GFH was investigated as a function of contact time (1 min to 24 h) at two different initial perchlorate concentrations (5 and 10 mg L<sup>-1</sup>). It was noticed that perchlorate removal increased with time (Fig. 1). The trends of the plots in Fig. 1 exhibit that perchlorate uptake was rapid in the beginning followed by a slower removal that gradually reached a plateau. Maximum removal of perchlorate was achieved within the first 30 min of contact time and equilibrium was attained in 60 min. There was no significant change in perchlorate uptake by GFH in the following 24 h. A similar trend of fast kinetics was observed during

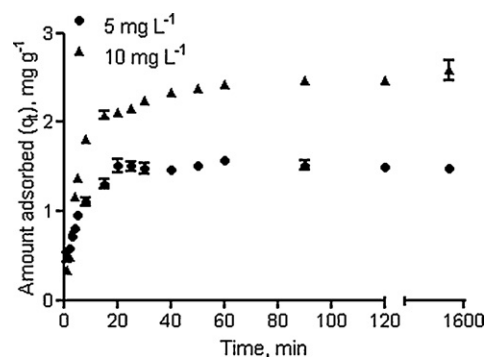


Fig. 1. Effect of contact time and initial perchlorate concentration on adsorption of perchlorate on GFH (temperature = 25  $^{\circ}$ C, GFH dose = 1 g L<sup>-1</sup>). Error bars show the standard deviation from triplicates.

**Table 1**  
Comparison of pseudo-first-order, pseudo-second-order, Weber and Morris and Bangham's models parameters, and calculated  $q_{e(\text{cal})}$  and experimental  $q_{e(\text{exp})}$  values for different initial perchlorate concentrations.

$C_0$ (mg L <sup>-1</sup> )	$q_{e(\text{exp})}$ (mg g <sup>-1</sup> )	$k_f \times 10^{-1}$ (min <sup>-1</sup> )	$q_{e(\text{cal})}$ (mg g <sup>-1</sup> )	$R^2$
Pseudo-first-order model				
5	1.45	1.06	1.18	0.978
10	2.45	0.89	1.85	0.942
$C_0$ (mg L <sup>-1</sup> )	$q_{e(\text{exp})}$ (mg g <sup>-1</sup> )	$k_s \times 10^{-1}$ (g mg <sup>-1</sup> min <sup>-1</sup> )	$q_{e(\text{cal})}$ (mg g <sup>-1</sup> )	$R^2$
Pseudo-second-order model				
5	1.45	1.59	1.64	0.998
10	2.45	0.81	2.62	0.999
$C_0$ (mg L <sup>-1</sup> )	$k_{ip1}$ (mg g <sup>-1</sup> min <sup>-0.5</sup> )	$R^2$	$k_{ip2}$ (mg g <sup>-1</sup> min <sup>-0.5</sup> )	$R^2$
Weber and Morris model				
5	0.39	0.993	0.22	0.992
10	0.87	0.949	0.17	0.963
$C_0$ (mg L <sup>-1</sup> )	$k_0$ (mL (g L <sup>-1</sup> ) <sup>-1</sup> )	$\alpha$	$R^2$	
Bangham's model				
5	0.02	0.40	0.986	
10	0.01	0.62	0.918	

the adsorption of several other anions (e.g. bromate, fluoride and arsenic,) onto GFH [30,31,35].

The effect of initial perchlorate concentration on equilibrium adsorption was also investigated at two different initial perchlorate concentrations (5 and 10 mg L<sup>-1</sup>). Perchlorate uptake by GFH increased when the initial perchlorate concentration increased from 5 to 10 mg L<sup>-1</sup> (Fig. 1). This behavior can be explained due to the increase in the driving force of the concentration gradient, as an increase in the initial perchlorate concentration. Such phenomenon is common in a batch reactor with either constant adsorbent dose or varying initial adsorbate concentration or vice versa [36].

### 3.2. Kinetic modeling

In order to investigate the adsorption mechanism of perchlorate on GFH, four kinetic models were applied namely, pseudo-first-order (Supporting information, Section 1), pseudo-second-order (Section 3.2.1), Weber and Morris intraparticle diffusion model (Section 3.2.2) and Bangham's pore diffusion models (Supporting information, Section 2). The applicable models have been discussed in detail below and modeling parameters are provided in Table 1.

#### 3.2.1. Pseudo-second-order kinetic model

The adsorption kinetics was described as pseudo-second-order process [37]. It can be represented in the following form:

$$\frac{t}{q_t} = \frac{1}{k_s q_e^2} + \frac{1}{q_e} t \quad (2)$$

where,  $q_e$  and  $q_t$  are the amount of perchlorate adsorbed on GFH (mg g<sup>-1</sup>) at equilibrium and at time  $t$  (min), respectively, and  $k_s$  is the rate constant for the pseudo-second-order kinetic model. The equilibrium adsorption capacity,  $q_{e(\text{cal})}$  and  $k_s$  were determined from the slope and intercept of plot of  $t/q_t$  versus  $t$  (Fig. 2(A)) and are compiled in Table 1. The plots were found to be linear with good correlation coefficients (0.998 and 0.999 for 5 and 10 mg L<sup>-1</sup> initial perchlorate concentration, respectively) and the theoretical  $q_{e(\text{cal})}$  values agree well to the experimental  $q_{e(\text{exp})}$  values at two concentrations studied. This implies that the pseudo-second-order model is in good agreement with experimental data and can be used to favorably explain the perchlorate adsorption on GFH.

#### 3.2.2. Weber and Morris intraparticle diffusion model

The intraparticle diffusion approach described by Weber and Morris [38] can be used to predict if intraparticle diffusion is the rate-limiting step which is given by Eq. (3):

$$q_t = k_{ip} t^{1/2} + C \quad (3)$$

where,  $k_{ip}$  is intraparticle diffusion rate constant and  $C$  is the intercept related to the thickness of the boundary layer. According to Eq. (3), a plot of  $q_t$  versus  $t^{1/2}$  should be a straight line if the adsorption mechanism follows the intraparticle diffusion process only. However, if the data exhibit multi-linear plots, then the process is governed by two or more steps. The Weber and Morris plots of

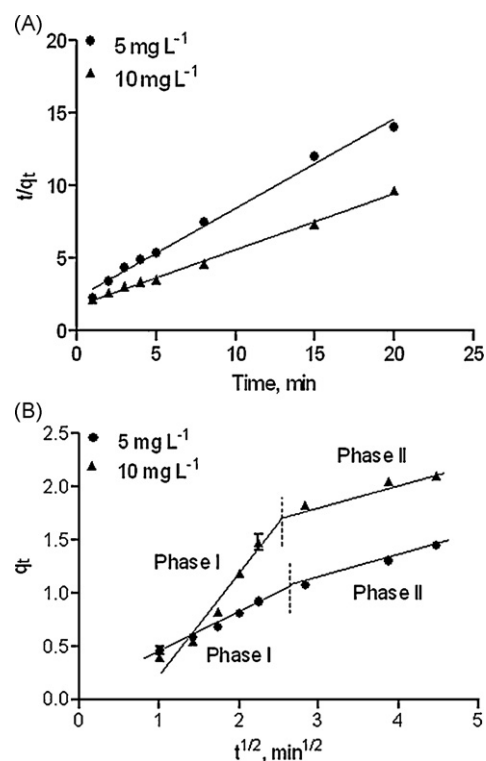


**Fig. 2.** Kinetic modeling of adsorption of perchlorate on GFH (A) pseudo-second-order kinetic plots; (B) Weber and Morris intraparticle diffusion plots. Error bars show the standard deviation from triplicates.

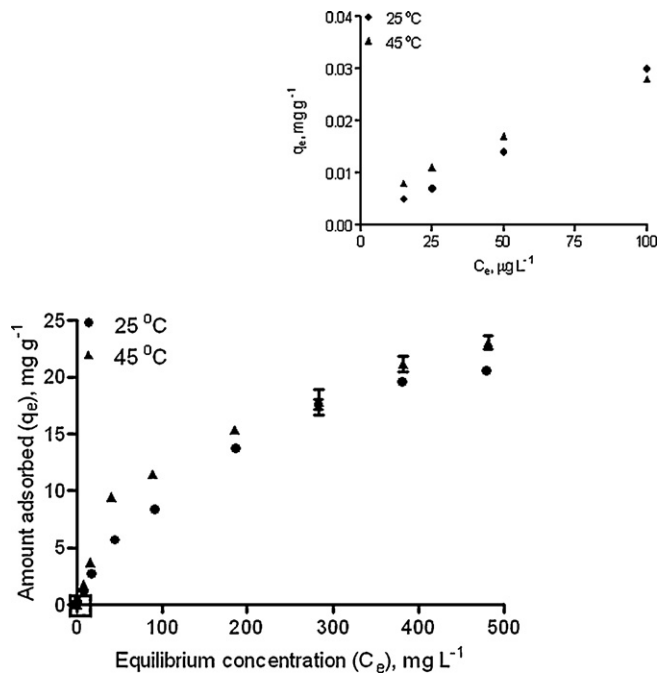


**Fig. 3.** Adsorption isotherms of perchlorate adsorption on GFH (contact time = 24 h, GFH dose = 1 g L<sup>-1</sup>) (The figure in inset shows the data points at lower perchlorate concentration ( $\mu\text{g L}^{-1}$ ) range of the isotherm.) Error bars show the standard deviation from triplicates.

perchlorate adsorption on GFH are shown in Fig. 2(B). Two separate zones can be clearly seen in the figure. The first linear portion (phase I) at both concentrations, can be attributed to the immediate utilization of the most readily available adsorbing sites on the adsorbent surface. Phase II may be attributed to very slow diffusion of the adsorbate from the surface site into the inner pores. Thus, initial portion of perchlorate adsorption by GFH may be governed by the initial intraparticle transport of perchlorate controlled by surface diffusion process and the later part controlled by pore diffusion. The values of  $k_{ip1}$  and  $k_{ip2}$  (diffusion rate constants for phase I and II, respectively) obtained from the slope of linear plots are listed in Table 1. Higher values of  $k_{ip1}$  as compared to  $k_{ip2}$  in both cases are indicative of the rapid initial step (phase I) which is followed by a slow step (phase II). The deviation of the straight lines in Weber and Morris model may be due to the difference in the rate of mass transfer in initial and final stages of adsorption [39].

### 3.3. Adsorption isotherms

In order to evaluate the adsorption capacity of GFH for perchlorate, the equilibrium adsorption of perchlorate was studied as a function of perchlorate concentration (50  $\mu\text{g L}^{-1}$  to 500  $\text{mg L}^{-1}$ ) and the adsorption isotherms are shown in Fig. 3. The equilibrium was not achieved in the lower perchlorate concentration range ( $\mu\text{g L}^{-1}$ ) (as shown in the inset of Fig. 3). Thus, higher concentrations (in  $\text{mg L}^{-1}$  level) of perchlorate were chosen to attain equilibrium and

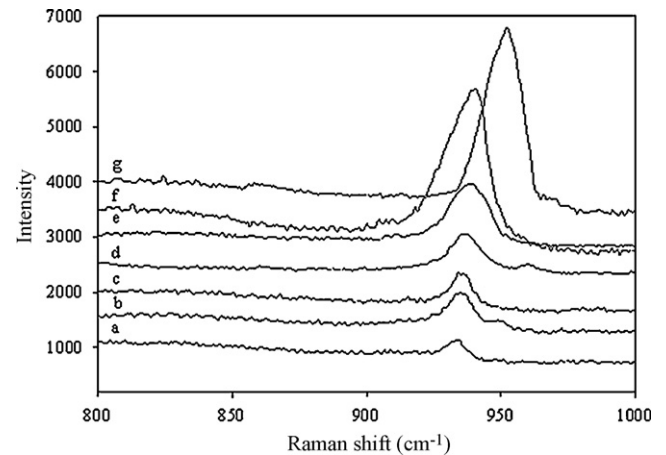


**Fig. 4.** Raman spectra of perchlorate-sorbed GFH samples ((a) 20  $\text{mg L}^{-1}$ ; (b) 50  $\text{mg L}^{-1}$ ; (c) 100  $\text{mg L}^{-1}$ ; (d) 200  $\text{mg L}^{-1}$ ; (e) 500  $\text{mg L}^{-1}$ ; (f) 700  $\text{mg L}^{-1}$  perchlorate-sorbed on GFH; (g) sodium perchlorate).

to know the maximum adsorption potential of GFH for perchlorate removal. An adsorption capacity of ca. 20.0  $\text{mg g}^{-1}$  was observed for perchlorate on GFH at pH 6.0–6.5 at 25 °C. The initial sharp rise in the isotherm indicates the availability of readily accessible sites for adsorption. However, site saturation occurs as the perchlorate concentration increases and a plateau is reached indicating that no more sites remain available for adsorption. Adsorption potential of GFH from the present study was compared with previously reported adsorbents for perchlorate removal and compiled in Table 2. It is evident that GFH shows efficient adsorption capacity for perchlorate removal from water.

In order to investigate the effect of temperature on perchlorate removal by GFH, adsorption experiments were also performed at 45 °C. A comparison of adsorption isotherms at 25 and 45 °C indicates that perchlorate sorption by GFH was not significantly affected by increase in the temperature (Fig. 3). Similar results were also reported for perchlorate removal using protonated cross-linked chitosan [25].

### 3.4. Raman spectroscopic analysis

Raman spectroscopic analysis was conducted to provide an insight into the mechanism of perchlorate adsorption by GFH. A range of perchlorate solution (20, 50, 100, 200, 500, and 700  $\text{mg L}^{-1}$ ) was equilibrated with GFH and the perchlorate-sorbed GFH samples were analyzed with Raman spectroscopy. It has been reported that sodium perchlorate exhibits a peak at 952  $\text{cm}^{-1}$  indicating the bonding environment of perchlorate in the solid is quite different from that of free perchlorate ion in the solution [40]. The concentrated aqueous solution of perchlorate has characteristic peaks at 941  $\text{cm}^{-1}$  whereas, the 1000  $\text{mg L}^{-1}$   $\text{NaClO}_4$  aqueous solution has a characteristic perchlorate peak at 933  $\text{cm}^{-1}$  [40,41].

The Raman spectra of perchlorate-sorbed GFH samples (Fig. 4) indicate that the intensity of  $\nu_1$  symmetric stretching is the func-

**Table 2**  
Comparison of perchlorate adsorption on various adsorbents.

Adsorbent	Perchlorate adsorbed	Reference
Ammonia tailored activated carbons	7.3–9.0 $\text{mg g}^{-1}$	[23]
Protonated cross-linked chitosan	45.45 $\text{mg g}^{-1}$	[25]
Filtrisorb F400	0.32 $\text{mmol g}^{-1}$	[26]
Nuchar SN	0.19 $\text{mmol g}^{-1}$	[26]
GAC preloaded with iron and an organic complex solution	0.336 $\text{mg g}^{-1}$	[48]
Surfactant-modified zeolite	40–47 $\text{mmol kg}^{-1}$	[49]
GFH	~20.0 $\text{mg g}^{-1}$	Present study

**Table 3**  
Langmuir and Freundlich constants for the adsorption of perchlorate on GFH at different temperatures.

Temperature (°C)	Langmuir constants				Freundlich constants		
	$q_m$ (mg g <sup>-1</sup> )	$b$ (L mol <sup>-1</sup> )	$R_L$	$R^2$	$1/n$	$K_F$ (mg g <sup>-1</sup> ) (L mg <sup>-1</sup> ) <sup>1/n</sup>	$R^2$
25	20.12	$0.09 \times 10^4$	0.48	0.992	0.61	0.55	0.991
45	23.47	$0.10 \times 10^4$	0.46	0.996	0.62	1.07	0.944

tion of concentration of perchlorate. The symmetric ( $\nu_1$ ) mode of perchlorate ion on GFH was observed in the range of 934–941 cm<sup>-1</sup>. The  $\nu_1$  symmetric stretching mode of the anion is due to ion association or ion–ion interactions [42]. Raman shift were observed at 934–935 cm<sup>-1</sup> for the adsorption of 20, 50, and 100 mg L<sup>-1</sup> perchlorate solution on GFH. The red shift of 18 cm<sup>-1</sup> from 952 cm<sup>-1</sup> clearly indicates that the interaction between perchlorate ion and GFH is much stronger than physisorption and perchlorate forms outer sphere complexes due to strong electrostatic attraction with GFH. Gu et al. [43] investigated Raman spectroscopy of perchlorate at low concentration and suggested the symmetric Raman shift of perchlorate at 930 cm<sup>-1</sup> (a red shift of 22 cm<sup>-1</sup> from 952 cm<sup>-1</sup>) is due to the strong electrostatic interaction between perchlorate and quaternary ammonium functionalized resin.

A further shift in Raman shift from 935 to 941 cm<sup>-1</sup> on increasing the concentration of perchlorate (200, 500 and 700 mg L<sup>-1</sup>) suggests that perchlorate is also present in the diffused swarm layer. Adsorption of 700 mg L<sup>-1</sup> perchlorate on GFH resulted in a relatively intense peak with Raman shift 941 cm<sup>-1</sup>, in comparison with 200 and 500 mg L<sup>-1</sup> perchlorate (Raman shift 937 and 939 cm<sup>-1</sup>), presumably due to the higher number of perchlorate ions adsorbed on the surface of GFH. The broadening of Raman peaks for 500 and 700 mg L<sup>-1</sup> is thought to result from co-elution of two peaks: one for outer sphere complexation and the other due to the presence of perchlorate in diffused swarm layer.

The Raman spectroscopic data suggest the dominance of electrostatic interaction between perchlorate and GFH surface. Perchlorate sorption onto iron oxides has been proposed to occur through nonspecific outer sphere electrostatic interactions where electrostatic contributions to the free energy of adsorption dominate [44]. The perchlorate anion will retain its primary hydration shell, i.e. at least one water molecule is interposed between the anion and the surface [44]. This type of adsorption on iron oxides tends to result in easy displacement of perchlorate by other co-anions present in the groundwater. The occurrence of perchlorate in the diffused swarm layer at higher anion concentration suggests saturation of sites in the outer sphere layer by perchlorate.

### 3.5. Isotherm modeling

The adsorption data was further analyzed using two isotherm models, viz. Freundlich (Supplementary information, Section 3) and Langmuir models. The Langmuir [45] model can be described by following equation:

$$\frac{1}{q_e} = \frac{1}{q_m} + \frac{1}{q_m b C_e} \quad (4)$$

where,  $q_e$  is amount adsorbed at equilibrium concentration  $C_e$ ,  $q_m$  is the Langmuir constant representing maximum monolayer adsorption capacity and  $b$  is the Langmuir constant related to energy of adsorption. The plots of  $1/q_e$  as a function of  $1/C_e$  for the adsorption of perchlorate on GFH are shown in Fig. 5. The plots were found linear with good correlation coefficients (>0.99) indicating the applicability of Langmuir model in the present study. The values of monolayer capacity ( $q_m$ ) and Langmuir constant ( $b$ ) are given in Table 3. The values of  $q_m$  calculated by the Langmuir isotherm were all close to experimental values at given temperatures. These facts suggest that perchlorate is adsorbed in the form of monolayer

coverage on the surface of the adsorbent. The sorption isotherms of anions on iron oxides typically follow Langmuirian behavior as described by previous researchers [44].

The influence of adsorption isotherm shape has been discussed [46] to examine whether adsorption is favorable in terms of ' $R_L$ ', a dimensionless constant referred to as separation factor or equilibrium parameter. ' $R_L$ ' is calculated using the following equation:

$$R_L = \frac{1}{1 + bC_0} \quad (5)$$

The  $R_L$  values obtained are compiled in Table 3. Both the  $R_L$  values lie between 0 and 1 confirming that the adsorption isotherm is favorable.

### 3.6. Thermodynamic parameters

The nature and thermodynamic feasibility of the sorption process were determined by evaluating the thermodynamic constants, standard free energy ( $\Delta G^\circ$ ), standard enthalpy ( $\Delta H^\circ$ ) and standard entropy ( $\Delta S^\circ$ ) using the following equations:

$$\Delta G^\circ = -RT \ln(K) \quad (6)$$

$$\ln\left(\frac{K_2}{K_1}\right) = -\frac{\Delta H^\circ}{R} \left(\frac{1}{T_2} - \frac{1}{T_1}\right) \quad (7)$$

$$\Delta G^\circ = \Delta H^\circ - T\Delta S^\circ \quad (8)$$

where,  $R$  is the universal gas constant (8.314 J mol<sup>-1</sup> K<sup>-1</sup>),  $T$  is the temperature in Kelvin and  $K$  is the equilibrium constant. The adsorption process is spontaneous in nature, as indicated by the negative value of  $\Delta G^\circ$  (-26.8 kJ mol<sup>-1</sup>). The positive value of  $\Delta H^\circ$  for perchlorate adsorption is 4.15 kJ mol<sup>-1</sup>, suggesting that the interaction of perchlorate and GFH is endothermic in nature. Affinity of the adsorbent for perchlorate is represented by the positive value of  $\Delta S^\circ$  (103.87 J mol<sup>-1</sup> K<sup>-1</sup>).

### 3.7. Effect of pH and competing anions on perchlorate sorption by GFH

The sorption of perchlorate ( $C_0$ : 20 mg L<sup>-1</sup>) on GFH was investigated at different pH ranging from 3 to 12 and results are shown in Fig. 6. The optimum perchlorate removal was observed at pH range 3.0–7.0. As the pH increased beyond 8, the removal of perchlorate by GFH was decreased. The low adsorption of perchlorate at higher

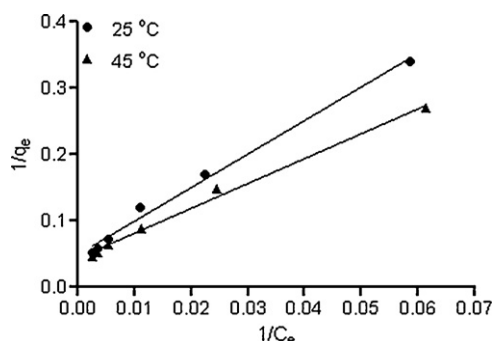
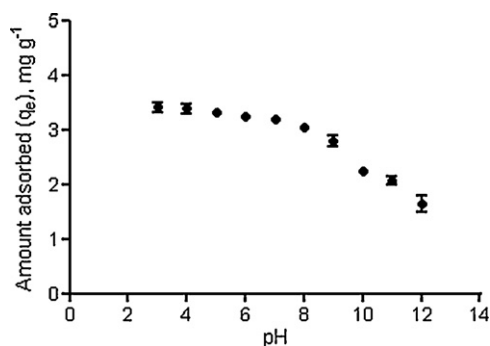
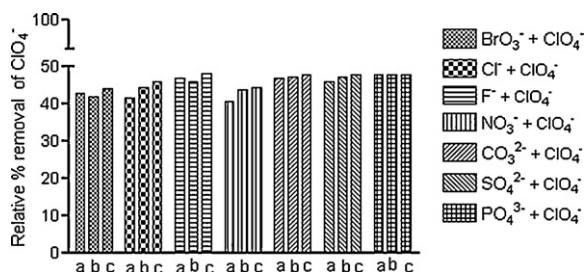


Fig. 5. Langmuir isotherms of perchlorate adsorption on GFH.



**Fig. 6.** Effect of pH on perchlorate adsorption on GFH ( $C_0 = 20 \text{ mg L}^{-1}$ , temperature =  $25^\circ\text{C}$ , contact time = 24 h, GFH dose =  $1 \text{ g L}^{-1}$ ). Error bars show the standard deviation from triplicates.



**Fig. 7.** Effect of different concentrations of competitive anions on perchlorate adsorption on GFH (temperature =  $25^\circ\text{C}$ , contact time = 24 h, GFH dose =  $1 \text{ g L}^{-1}$ ) ((a)  $20 \text{ mg L}^{-1}$ ; (b)  $50 \text{ mg L}^{-1}$ ; (c)  $100 \text{ mg L}^{-1}$ ).

pH might be due to the electrostatic repulsion of perchlorate by the negatively charged GFH surface at high pH.

The impact of various anions including chloride ( $\text{Cl}^-$ ), fluoride ( $\text{F}^-$ ), bromate ( $\text{BrO}_3^-$ ), nitrate ( $\text{NO}_3^-$ ), sulphate ( $\text{SO}_4^{2-}$ ), carbonate ( $\text{CO}_3^{2-}$ ) and phosphate ( $\text{PO}_4^{3-}$ ) on perchlorate removal by GFH, was investigated at  $20 \text{ mg L}^{-1}$  of initial perchlorate concentration. The concentration of competing anions was varied from 20 to  $100 \text{ mg L}^{-1}$  (Fig. 7). Anions present in the perchlorate solutions are likely to limit the perchlorate removal efficiency. In the presence of chloride, nitrate and bromate, percent removal of perchlorate was ca. 43%, while in case of other anions (fluoride, sulphate, phosphate and carbonate), percent removal of perchlorate was ca. 47%. There was no significant change in the percent removal of perchlorate under the three investigated concentrations (20, 50, and  $100 \text{ mg L}^{-1}$ ) of competing anions. It has been reported that perchlorate can be displaced by the occurrence of preferred anion viz. phosphate, fluoride and even chloride [47] by the protonated mineral surfaces, which is in agreement with the present results.

#### 4. Conclusions

The results of the present work suggest that GFH can be used as a promising alternative for perchlorate removal from aqueous solutions. The adsorption capacity of GFH for perchlorate was ca.  $20.0 \text{ mg g}^{-1}$  at  $25^\circ\text{C}$ . The adsorption isotherms were fitted well with Langmuir model. Kinetic analyses indicate that the adsorption process followed a pseudo-second-order kinetics under the selected concentration range. The optimum perchlorate removal was observed at pH range 3.0–7.0. The Raman spectroscopy results are in agreement with the fact that perchlorate bonds through electrostatic interactions on the iron surfaces, and as the perchlorate concentration increases, the anion shift into the diffused swarm layer. Experimental data can be further used to guide and optimize pilot scale experiments that can enable the commercial exploitation of GFH for perchlorate removal from water.

#### Acknowledgements

Authors are grateful to 21st Frontier research project (Sustainable Water Resources Research Center 3-4-3), Brain Korea-21 (BK-21) program of Ministry of Education, Global Research Laboratory (GRL) project by Korean Institute of Geoscience and Mineral Resources (KIGAM), NP2008-019, and Agency for Defense Development (ADD) research fund for financial support.

#### Appendix A. Supplementary data

Supplementary data associated with this article can be found, in the online version, at doi:10.1016/j.cej.2010.02.043.

#### References

- [1] US Environmental Protection Agency (US EPA), EPA report, Perchlorate Environmental Contamination: Toxicological Review and Risk Characterization, external review draft, 2002.
- [2] Y. Shi, P. Zhang, Y. Wang, J. Shi, Y. Cai, S. Mou, G. Jiang, Perchlorate in sewage sludge, rice, bottled water and milk collected from different areas in China, *Environ. Int.* 33 (2007) 955–962.
- [3] O. Quinones, J. Oh, B. Vanderford, J.H. Kim, J. Cho, S.A. Snyder, Perchlorate assessment of the Nakdong and Yeongsan watersheds, Republic of Korea, *Environ. Toxicol. Chem.* 26 (2007) 1349–1354.
- [4] K. Kosaka, M. Asami, Y. Matsuoka, M. Kamoshita, S. Kunikane, Occurrence of perchlorate in drinking water sources of metropolitan area in Japan, *Water Res.* 41 (2007) 3473–3482.
- [5] E.T. Urbansky, Perchlorate chemistry: implications for analysis and remediation, *Bioremed. J.* 2 (1998) 81–95.
- [6] ITRC (Interstate Technology Regulatory Council), Perchlorate: Overview of issues, status, and remedial options, 2005. <http://www.itrcweb.org/Documents/PERC-1.pdf> (accessed on 15/08/09).
- [7] R. Renner, Perchlorate rockets to US national attention, *J. Environ. Monitor.* 1 (1999) 37–38.
- [8] E.T. Urbansky, S.K. Brown, M.L. Magnuson, C.A. Kelty, Perchlorate levels in samples of sodium nitrate fertilizer derived from Chilean caliche, *Environ. Pollut.* 112 (2001) 299–302.
- [9] GAO (U.S. Government Accountability Office), Perchlorate: A system to track sampling and cleanup results is needed, GAO-05-462, 2005.
- [10] NAS (National Research Council of the National Academies), Health implications of perchlorate ingestion, 2005.
- [11] NIOSH (National Institute for Occupational Safety and Health), 2007. <http://www.cdc.gov/niosh/ipcs/nicstart.html> (accessed on 18/08/09).
- [12] Z. Li, F.X. Li, D. Byrd, G.M. Deyhle, D.E. Sesser, M.R. Skeels, S.H. Lamm, Neonatal thyroxine level and perchlorate in drinking water, *J. Occup. Environ. Med.* 42 (2000) 200–205.
- [13] K.S. Crump, J.P. Gibbs, Benchmark calculations for perchlorate from three human cohorts, *Environ. Health Perspect.* 113 (2005) 1001–1008.
- [14] US Environmental Protection Agency (US EPA), Drinking water contaminant list, EPA document No. 815-F-98-002, GPO, Washington, DC, 1998.
- [15] US Environmental Protection Agency (US EPA), EPA news release, 2005. <http://yosemite.epa.gov/opa/admpress.nsf/0/c1a57d2077c4bfda85256fac005b8b32?OpenDocument> (accessed on 20/08/09).
- [16] J. Xu, Y. Song, B. Min, L. Steinberg, B.E. Logan, Microbial degradation of perchlorate: principles and applications, *Environ. Eng. Sci.* 20 (2003) 405–422.
- [17] X. Yu, C. Amrhein, M.A. Deshusses, M.R. Matsumoto, Perchlorate reduction by autotrophic bacteria in the presence of zero-valent iron, *Environ. Sci. Technol.* 40 (2006) 1328–1334.
- [18] X. Yu, C. Amrhein, M.A. Deshusses, M.R. Matsumoto, Perchlorate reduction by autotrophic bacteria attached to zerovalent iron in a flow-through reactor, *Environ. Sci. Technol.* 41 (2007) 990–997.
- [19] B. Gu, G.M. Brown, C.C. Chiang, Treatment of perchlorate-contaminated groundwater using highly selective, regenerable ion-exchange technologies, *Environ. Sci. Technol.* 41 (2007) 6277–6282.
- [20] V. Roquebert, S. Booth, R.S. Cushing, G. Crozes, E. Hansen, Electrodialysis reversal (EDR) and ion exchange as polishing treatment for perchlorate treatment, *Desalination* 131 (2000) 285–291.
- [21] M.Y. Rusanova, P. Polášková, M. Muzikaf, W.R. Fawcett, Electrochemical reduction of perchlorate ions on platinum-activated nickel, *Electrochim. Acta* 51 (2006) 3097–3101.
- [22] R. Parette, F.S. Cannon, The removal of perchlorate from groundwater by activated carbon tailored with cationic surfactants, *Water Res.* 39 (2005) 4020–4028.
- [23] W. Chen, F.S. Cannon, J.R. Rangel-Mendez, Ammonia-tailoring of GAC to enhance perchlorate removal II: perchlorate adsorption, *Carbon* 43 (2005) 581–590.
- [24] I.-H. Yoon, X. Meng, C. Wang, K.-W. Kim, S. Bang, E. Choe, L. Lippincott, Perchlorate adsorption and desorption on activated carbon and anion exchange resin, *J. Hazard. Mater.* 164 (2009) 87–94.

- [25] Y. Xie, S. Li, F. Wang, G. Liu, Removal of perchlorate from aqueous solution using protonated cross-linked chitosan, *Chem. Eng. J.* 156 (2010) 56–63.
- [26] R. Mahmudov, C.P. Huang, Perchlorate removal by activated carbon adsorption, *Sep. Purif. Technol.* 70 (2010) 329–337.
- [27] X.-H. Guan, J. Wang, C.C. Chusuei, Removal of arsenic from water using granular ferric hydroxide: macroscopic and microscopic studies, *J. Hazard. Mater.* 156 (2008) 178–185.
- [28] M. Jang, F.S. Cannon, R.B. Parette, S.-J. Yoon, W. Chen, Combined hydrous ferric oxide and quaternary ammonium surfactant tailoring of granular activated carbon for concurrent arsenate and perchlorate removal, *Water Res.* 43 (2009) 3133–3143.
- [29] W. Driehaus, Arsenic removal-experience with the GEH process in Germany, *Water Supply* 2 (2002) 275–280.
- [30] A. Bhatnagar, Y. Choi, Y. Yoon, Y. Shin, B.H. Jeon, J.W. Kang, Bromate removal from water by granular ferric hydroxide (GFH), *J. Hazard. Mater.* 170 (2009) 134–140.
- [31] E. Kumar, A. Bhatnagar, M. Ji, W. Jung, S. Lee, S.J. Kim, G. Lee, H. Song, J.Y. Choi, J. Yang, B.H. Jeon, Defluoridation from aqueous solutions by granular ferric hydroxide (GFH), *Water Res.* 43 (2009) 490–498.
- [32] A. Genz, B. Baumgarten, M. Goernitz, M. Jekel, NOM removal by adsorption onto granular ferric hydroxide: equilibrium, kinetics, filter and regeneration studies, *Water Res.* 42 (2008) 238–248.
- [33] M. Badruzzaman, P. Westerhoff, D.R.U. Knappe, Intraparticle diffusion and adsorption of arsenate onto granular ferric hydroxide (GFH), *Water Res.* 38 (2004) 4002–4012.
- [34] M. Steiner, W. Pronk, M.A. Boller, Modeling of copper sorption onto GFH and design of full-scale GFH adsorbers, *Environ. Sci. Technol.* 40 (2006) 1629–1635.
- [35] K. Banerjee, G.L. Amy, M. Prevost, S. Nour, M. Jekel, P.M. Gallagher, C.D. Blumenschein, Kinetic and thermodynamic aspects of adsorption of arsenic onto granular ferric hydroxide (GFH), *Water Res.* 42 (2008) 3371–3378.
- [36] K.H. Chu, Removal of copper from aqueous solution by chitosan in prawn shell: adsorption equilibrium and kinetics, *J. Hazard. Mater.* B90 (2002) 77–95.
- [37] Y.S. Ho, G. McKay, Pseudo-second-order model for sorption processes, *Process Biochem.* 34 (1999) 451–465.
- [38] W.J. Weber Jr., J.C. Morris, Kinetics of adsorption on carbon from solution, *J. Sanit. Eng. Div.* 89 (1963) 31–59.
- [39] K.K. Panday, G. Prasad, V.N. Singh, Mixed adsorbent for Cu(II) removal from aqueous solutions, *Environ. Technol. Lett.* 50 (1986) 547–554.
- [40] A.G. Miller, J.W. Macklin, Chlorine-35 nuclear magnetic resonance study of aqueous sodium perchlorate association, *J. Phys. Chem.* 89 (1985) 193–1201.
- [41] R.E. Hester, R.A. Plane, Metal-oxygen bonds in complexes: Raman spectra of tris-acetylacetonato and trisoxalato complexes of aluminum, gallium, and indium, *Inorg. Chem.* 3 (1964) 769–770.
- [42] R.A. Silva, G.G. Silva, M.A. Pimenta, Micro-Raman study of polydioxolane/LiClO<sub>4</sub> and NaClO<sub>4</sub> electrolytes, *Appl. Phys. Lett.* 67 (1995) 3352–3354.
- [43] B. Gu, J. Tio, W. Wang, Y. Ku, S. Dai, Raman spectroscopic detection for perchlorate at low concentrations, *Appl. Spectrom.* 58 (2004) 741–744.
- [44] R.M. Cornell, U. Schwertmann, *The Iron Oxides: Structure, Properties, Reactions, Occurrences, and Uses*, Wiley-VCH Publishers, Weinheim, 2003.
- [45] I. Langmuir, The constitution and fundamental properties of solids and liquids, part I; solids, *J. Am. Chem. Soc.* 38 (1916) 2221–2295.
- [46] T.W. Weber, R.K. Chakravorti, Pore and solid diffusion models for fixed bed adsorbents, *J. Am. Inst. Chem. Eng.* 20 (1974) 228–238.
- [47] E.T. Urbansky, T.W. Collette, Comparison and evaluation of laboratory performance on a method for the determination of perchlorate in fertilizers, *J. Environ. Monit.* 3 (2001) 454–462.
- [48] F.S. Cannon, C. Na, Perchlorate removal using tailored granular activated carbon and chemical regeneration, in: *Perchlorate Workshop of the Pollution Prevention Technology Transfer Conference of the Joint Armed Services*, San Antonio, TX, August 23–24, 2000.
- [49] P. Zhang, D.M. Avudzeza, R.S. Bowman, Removal of perchlorate from contaminated waters using surfactant-modified zeolite, *J. Environ. Qual.* 36 (2007) 1069–1075.